IBIS/PICsIT Instrument Specific Software Scientific Validation Report

Luigi Foschini
INTEGRAL – IBIS Team
Istituto di Astrofisica Spaziale e Fisica Cosmica (IASF) del CNR
Sezione di Bologna, Italy

Version 4.0

July 8, 2004

	Revision History
v 1.0	First version for first software release of March 2003.
28/02/2003	
v 1.1	Update for the intermediate software release of May 2003.
30/04/2003	Early analysis of Cyg X–1, cleaning of cosmic–ray induced events,
	improvement of the position accuracy, comparison with ECOE data.
v 1.2	Update for OSA 3 release.
27/10/2003	Crab in rev 102; automatic source location; timing analysis.
	Some error corrected. Removed the non–standard analysis section.
v 2.0	General reshape of the document style. Update for OSA 3.1 release.
02/02/2004	Updated the discussion on the uniformity maps and the inclusion of GTI.
v 4.0	Update for OSA 4 release (jump in the version number to match the OSA version).
06/07/2004	New executable for mosaic. New background maps.

1 Introduction

This report summarizes the scientific performances and reliability of the Instrument Specific Software (ISSW) of the PICsIT detector layer of the IBIS imager aboard INTEGRAL. The executables analysed here, together with their Instrument Configuration (IC) files, are those delivered by the IBIS Team to the ISDC for the integration in the Off–line Scientific Analysis (OSA) software package version 4.0 released by the ISDC to the public by July 2004. An equivalent report on the IBIS/ISGRI ISSW is provided in a separate document by A. Goldwurm et al. (IBIS/ISGRI Instrument Specific Software Scientific Validation Report).

The basic concepts of the scientific analysis of the IBIS telescope are described in Goldwurm et al. (2001, 2003), while more detailed technical information about the pipelines, data structures, tools, and complementary modules can be found in the documents *Introduction to INTEGRAL Data Analysis* (ISDC/OSA–INTRO), *ISDC Data Repository Organization* (ISDC/TEC013), and *IBIS Analysis User Manual* (ISDC/OSA–UM–IBIS).

This report provides a preliminary evaluation of the scientific performances of the IBIS/PICsIT software according to the tests performed so far. Further tests will be available in the next versions of the present document.

2 The IBIS/PICsIT data analysis

2.1 General concepts

The general purpose in the data analysis of astronomical instruments can be basically divided into two parts: the first, based on the analysis of images, is to measure the celestial coordinates, the spatial structure (extended or point–like sources), and the photometry of the source. The second, related to the study of the spectra, is to measure the flux and energy of emission/absorption lines, and the characteristics of the continuum. The measuring process adds several effects that contribute to modify the original image or spectrum. Therefore, it is necessary to operate corrections to the data in order to obtain an image/spectrum that is as much as possible consistent with the original one. Despite the differences depending on the instrument used in the observation, from a purely conceptual point of view, it is necessary to solve an inverse problem with distribution functions. In other words, by assuming for the sake of simplicity a monodimensional case, we have to solve the following integral equation of Fredholm of the first kind:

$$\phi(x) = \int \psi(z) K(x,z) dz \tag{1}$$

where ϕ is the observed density of probability function, while ψ is the corresponding original density of probability fuction that we want to restore. K is the kernel of the integral equation and represents the measuring process, including the effects of the measuring errors in the observed distribution. The kernel is called *point–spread function* (PSF) in the images, while it is called *line–spread function* (LSF) in the spectra. ϕ, ψ, and K are all non–negative functions, since they are connected with the density of the incoming photons.

The basic problem of the astronomical software is therefore "to clean" the PSF or LSF from all the systematic errors (including those of calibrations), before to proceed to the inversion of the integral equation. At the end of the correction ("cleaning") process, the kernel should contain only the statistical errors intrinsic to the measuring process. For example, in the case of a gaussian distribution with variance σ^2, the kernel is:

$$K(x,z) = \frac{1}{\sigma\sqrt{2\pi}} \exp \frac{-(x-z)^2}{2\sigma^2} \tag{2}$$

Depending on the type of instrument, there are different types of corrections. A system for astronomical data processing can be divided into three main steps, which in turn can be divided into sub–steps. The first step (**Level 0**) is the *preprocessing* level, where the telemetry coming from the satellite is unpacked and converted into a standard format (FITS) (see in the ISDC Technical Document section[1]). The basic data structure (RAW and PRP) is built, together with the On–Board Time (OBT) information, and the division into Science Windows (ScW) is set up (see ISDC/TEC013 for more details).

It is worth noting that, in the case of IBIS/PICsIT, there is also an on–board processing of the data before the Level 0, performed by the Hardware Event Preprocessor of IBIS (HEPI). This is necessary because of the limited telemetry available on–board the INTEGRAL satellite and the high count rate of background (≈ 3500 c/s) in the IBIS/PICsIT energy range ($0.17 - 10$ MeV). Therefore, HEPI performs a preliminary processing of the event list (containing the position y, z of the pixel, the channels $0 - 1023$, and the time information), before to send it to the ground. The corrections are: equalization by applying the gain and offset values of the HEPI look–up tables (LUT), conversion from channels to energy to reconstruct the multiple events, integration of events into histograms to save telemetry. The histograms are divided into two types: one (*spectral imaging*) is a data cube of $256 \times 64 \times 64$, containing still the full spatial information (64×64 pixel) and a moderate energy resolution (from the original 1024 to 256 channels). The integration time of a single histogram is generally corresponding to the duration of one ScW (≈ 2000 s), resulting in a loss of time information. Therefore, to perform time study, the other type of histogram (*spectral timing*) is designed to keep time resolution down to 1 ms, but with a great loss of energy resolution (from 1024 to 8 channels), and without spatial information. The combination of the *spectral imaging* and *spectral timing* is called *standard mode*. It is worth noting that IBIS/PICsIT can download directly the event list, without the integration on–board (*photon–by–photon* mode PPM), but with great consumption of telemetry. Therefore, with the exception of some observations of calibration, IBIS/PICsIT works only in standard mode, by producing spectral imaging histograms for single and multiple events, and histograms in spectral timing (default 4 energy bands and 2 ms of time resolution). More details on IBIS/PICsIT on–board processing are available in the IBIS User Manual, Issue 5.1.

Once the basic data structure is set up, there is the correction step (**Level 1**) where the instrument dependent corrections are applied. In this level, the OSA pipeline starts to work and perform the sublevels COR, DEAD, GTI, BIN_I/BIN_S, BKG_I/BKG_S. The specific corrections for IBIS/PICsIT are:

1. the intrinsic deadtime of the detector, that is the time during which it is not possible to process any event, since the detector is devoted to the processing of another event;
2. additional deviations from the on–board tables of gain and offset (only for PPM), and conversion from channels to energy;
3. filtering of the events according to the Good Time Intervals (GTI); for PPM only;
4. correction of partially downloaded histograms (for standard mode only);
5. correction for detector non–uniformities and subtraction of the background.

When the data are cleaned from background and corrected for instrumental effects, it is possible to move to the third level (**Level 2**), where the creation of images, spectra, and lightcurves is done (sublevels CAT_I/CAT_S, IMA/IMA2, SPE, LCR). The shadowgrams, produced in the previous level, are deconvolved according to the algorithms explained in Goldwurm et al. (2001, 2003), and the search for known sources is done, starting from a general catalog (Ebisawa et al. 2003). The attitude values of right

[1] Available at `http://isdc.unige.ch/index.cgi?Documents+doctec`.

ascension and declination obtained from the star tracker are referred to IBIS/PICsIT, by using a rotation and traslation (IBIS/PICsIT and the star tracker are not aligned). Moreover, the deconvolved image is projected into the sky with the gnomonic projection (TAN, cf Calabretta & Greisen 2002). The standard products of the source detection, performed on the sky images, is composed of the source coordinates and errors (in celestial coordinates and in pixels), the flux and its error (in counts per second), and the significance.

In the part of the extraction of the spectra, whose algorithms are still described in the seminal papers by Goldwurm et al. (2001, 2003), two IC files are of extreme importance. The first, named Auxiliary (or Ancillary) Response File (ARF) contains the information about the effective area of the detector as a function of the photon energy. The second IC file is named Redistribution Matrix File (RMF) and contains the information necessary to convert the counts into photons. This part is not yet included into OSA, since the RMF/ARF files are still missing.

The lightcurves are generated by using the spectral timing data, and therefore they are simply the count rates versus time for the whole detector. The deadtime and barycentric corrections are applied. The extraction of lightcurves for single point sources is not yet implemented, since it can be done only in PPM.

The output of the OSA pipeline can be analysed by means of the common software for high–energy astrophysics (e.g. Xspec, DS9, Xronos, ...).

2.2 General description of the executables

The IBIS/PICsIT–ISSW delivered to date for the Scientific Analysis of the PICsIT data include:

- `ibis_pics_deadtime` (v 2.4.1, 31 May 2004, DEAD level):
  to calculate the intrinsic deadtime of each semimodule of the detector. It is based on the use of a specific IBIS/PICsIT housekeeping, the *livetime counter*, that provides already the effective live time for each semimodule every 8 seconds. It provides also a display for the temperatures of each module.

- `ip_ev_correction` (v 1.6, 14 November 2002, COR level):
  to perform a correction of gain and offset variations in addition to those performed on board by HEPI. It is for data obtained in photon–by–photon mode. It is strilctly linked with the IC data structure `PICS-ENER-MOD`, containing the average gain, offset, and the deviations, pixel by pixel, from these values. Presently, no deviations are implemented, that is, only the onboard equalization are used.

- `ip_ev_shadow_build` (v 2.3, 14 January 2004, BIN_I/BIN_S level):
  to perform the building of the shadowgrams and the efficiency maps (dimensions 64×64) from data in photon–by–photon mode, according to energy bands or time bins selected by the user. The events are cleaned from the spurious events induced by cosmic-rays or noisy pixels and selected according to the available table of Good Time Intervals (GTI), which in turn are generated by another set of executables made by ISDC. See Sect. 3.2 for more details.

- `ip_si_shadow_build` (v 3.1, 31 May 2004, BIN_I/BIN_S level):
  to perform the building of shadowgrams and the efficiency maps (dimensions 64×64) from the data in standard mode (spectral imaging). It reads the binning tables from the IC file `PICS-BINT-CFG` (containing the data of the onboard HEPI LUT) and converts in channels the requested energy bands. By default, if histograms are not complete, the executable returns simply a warning, but it continues the analysis by discarding it. If the user wants to correct and use also partially downloaded histograms, it is possible to set the threshold

below which the executable correct (the missing pixels will be trated as killed pixels) and integrate the partially downloaded histograms. The parameter to set is `IBIS_IPS_corrPDH`, that has to be put equal to the maximum number of allowed missing cells. It is better to keep `IBIS_IPS_corrPDH`≤ 10000.

- `ip_shadow_ubc` (v 3.1, 24 March 2004, BKG_I/BKG_S level):
to perform the correction for background and detector non–uniformities. The output shadowgrams are also expanded to take into account the gaps between modules (from 64×64 to 65×67). The gaps and the killed pixels are filled with a mean value of counts averaged over the whole detector. There is also a variance map, calculated starting from the statistical variance of the detector counts and updated according to the correction performed (filled pixels, background subtraction, and so on...). The executable is linked with the following IC data structures: `PICS-SBAC-BKG` (background maps for single events), `PICS-MBAC-BKG` (background maps for multiple events), `PICS-SUNI-BKG` (detector non–uniformities for single events), and `PICS-MUNI-BKG` (detector non–uniformities for multiple events). See Sect. 3.1 for details.

- `ip_skyimage` (v 2.6, 18 March 2004, IMA2 level):
it performs the deconvolution and sky image reconstruction by means of the algorithm described by Goldwurm et al. (2003). The executable provides a basic deconvolved sky image, variance, and significance maps. For staring observation, it is possible to integrate the shadowgrams before the deconvolution and the automatic source location. For observations with dithering pattern, it is not possible to sum the shadowgrams before the deconvolution. Therefore, this module perform the basic deconvolution for every ScW. The weighted integration of the ScW images (mosaic) is the task of next executable.

- `ip_skymosaic` (v 1.2.1, 15 June 2004, CLEAN level):
it performs the integration of the individual ScW images into a single image (mosaic). It works mainly for dithering observations, but it can be used for staring pointings as well. For the moment, it is a very basic version, working for single events only, performing an integration with linear interpolation of the pixels, weight with the significance, and no automatic source detection. There are some problems in the selection of Scw with only multiple events or with no data.

- `ip_st_lc_extract` (v 2.3, 17 May 2004, LCR level):
it performs the extraction of the lightcurve of the whole detector from the spectral timing data. The barycentric correction is not applied, and the output should be processed with the OSA tool `barycent`.

It is worth noting that the IBIS/PICsIT ISSW makes use of other executables when inserted into the IBIS pipeline (creation and merging of GTI, Catalog Extraction, and so on...). These executables have been developed by ISDC people (N. Produit, R. Rolhfs, L. Lerusse) and are not analysed here directly, although the proper working of these modules is essential to have the full software package.

3 The correction for background

3.1 Maps

IBIS/PICsIT operates in an energy region dominated by the background (that is also higher than expected from numerical models – cf Ferguson et al. 2003), where we expect that the source counts are of the order of a few percent of the global counts detected. This means that the background correction is of paramount importance for the instrument capabilities.

The photons interacting with IBIS/PICsIT are distributed in a non–uniform way, because of several reasons (see Natalucci et al. 2003 for more details). The main effect is to produce an enhancement of counts at the edges of the modules and semimodules. Therefore, before to perform the deconvolution, it is necessary to flatten the detector non-uniformities and to correct for the background. Major improvements in the background maps are present in OSA4, with the availability of one set of maps with very long exposure. The IC files `pics_sbac_bkg_0007.fits` and `pics_mbac_bkg_0008.fits`) have been prepared by Piotr Lubinski by using the Core Programme data from revolution 49 to 67, for a global exposure of 1.7 Ms. It is possible to integrate a long number of Scw also from pointed observations, because in the energy range of PICsIT ($0.2 - 10$ MeV) there are a few sources. Moreover, by summing all the shadowgrams pixel by pixel, any possible contribution of sources is blurred. More details on background studies are available in the report by P. Lubinski and in the PICsIT instrument status report by Di Cocco et al. (in preparation).

One set of default energy bands has been created to have the best source statistics, with the lowest possible contamination from background or other events, such as the cosmic–rays induced events (see Segreto et al. 2003). These energy bands, prepared by G. Di Cocco and G. Malaguti, are shown in Table 1. It is worth noting that there was an update of the HEPI LUT during at the end of the revolution 169. The new binning table are slightly different from the previous one and led to some slight changes also in the energy bands (compare with Table 1 in the previous version of the present report). It is obvious that the user is free to select any type of energy band, but, in this case, he/she has also to built a new set of background maps.

Table 1: PICsIT Energy Bands. Columns: (1) Channel number in standard mode; (2) Energy [keV].

Channels Standard (1)	Energy (2)	Channels Standard (1)	Energy (2)
	Single Events		Multiple Events
$10 - 16$	$203 - 252$	$5 - 12$	$336 - 448$
$17 - 28$	$252 - 336$	$13 - 28$	$448 - 672$
$29 - 40$	$336 - 448$	$29 - 45$	$672 - 1036$
$41 - 56$	$448 - 672$	$45 - 74$	$1036 - 1848$
$57 - 82$	$672 - 1036$	$75 - 136$	$1848 - 3584$
$83 - 140$	$1036 - 1848$	$137 - 194$	$3584 - 6720$
$141 - 198$	$1848 - 3584$	$194 - 215$	$6720 - 9072$
$199 - 254$	$3584 - 6720$	$216 - 254$	$9072 - 13440$

Presently the executable contains two ways to rescale the background maps: according to the time of exposure and to the average value of counts. Although a more detailed study is necessary, it appears that the average value scaling could give better results. The distribution of significance values in the pixels of the field of view during the Crab observation of calibration is generally a gaussian, with a peak close to 0. A residual of $\pm 0.2\sigma$ is sometimes present. This systematic error will be corrected in the future versions of the software.

3.2 Cosmic–ray induced events – Noisy pixels

Since the beginning of the in–flight operations, it was clear that there were spurious events contaminating the detector in addition to the backgroud and source events([2]). The cause was identified in cosmic–ray induced events, that are roughly the 10% of the total events and affect mainly the energy bands below 300 keV (Segreto et al. 2003, see also Natalucci 2003). As underlined by Natalucci (2003) these fake events can significanly affect the performances of PICsIT. Moreover, there are also some noisy pixels (not hot pixels, that are killed by the onboard software), but it is not well known the origin of the noise

[2]See some nice animations by the IBIS Team in Tübingen at http://astro.uni–tuebingen.de/groups/integral/anim_gif/.

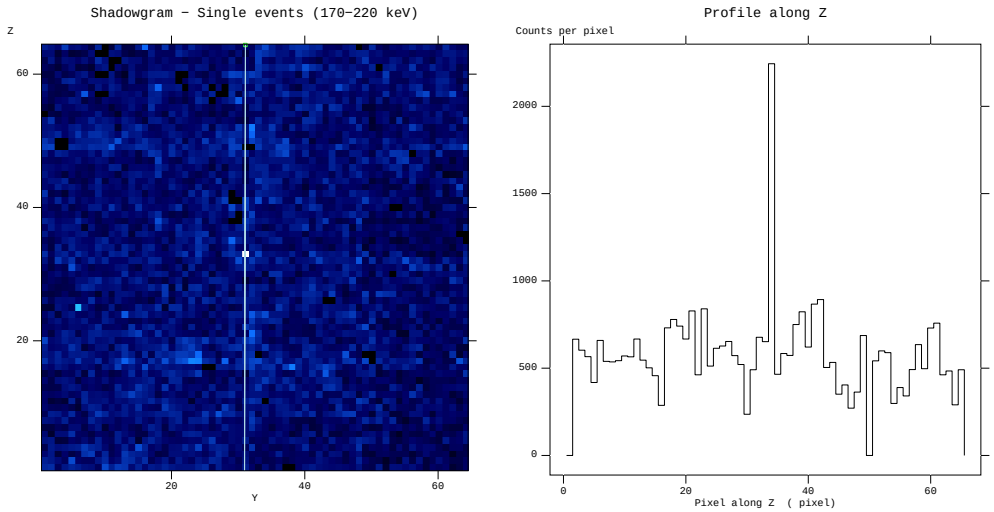

Figure 1: Effect of cosmic-rays induced events and/or noisy pixels on the shadowgrams. The white pixels have an anomalous high count value. This example is taken from the data of revolution 24 in the energy band $170 - 220$ keV; PICsIT was in photon–by–photon mode.

(electronics?). Anyway, the effect on the detector of these problems is the same: to produce pixels with anomalous counts (see Fig. 1).

File Edit Tools

	DELTA_TIME 1B	PICSIT_PHA 1I	PICSIT_Y 1B	PICSIT_Z 1B
1	123	30	45	22
2	128	25	54	62
3	130	35	36	4
4	132	30	15	9
5	133	39	11	56
6	139	40	62	33
7	141	39	31	57
8	146	24	13	18
9	150	24	13	18
10	152	24	13	18
11	154	25	13	18
12	156	24	13	18
13	157	28	31	20
14	159	24	13	18
15	163	24	13	18
16	164	24	13	18
17	166	24	13	18
18	167	73	42	48
19	167	26	2	24
20	176	28	19	3

Figure 2: Identification in the photon list (single events) of fake events produced by cosmic–rays and/or noisy pixels. Spurious events are emphasized in blue.

It is possible to perform a cleaning only in photon–by–photon mode, by acting on the single count. In standard mode, since only histograms are downloaded, an *a posteriori* correction is available: when the pixel counts are higher than a constant multiplied by the average count values, i.e. $counts > k \cdot average$, the pixel value is reset to the mean value. First tests showed a certain effectiveness of this correction, although the random nature of this type of correction introduces strong fluctuations in the count rates and significances in the reconstructed sky images.

This hypothesis is confirmed by the analysis of photon–by–photon data: indeed, in this case, it was

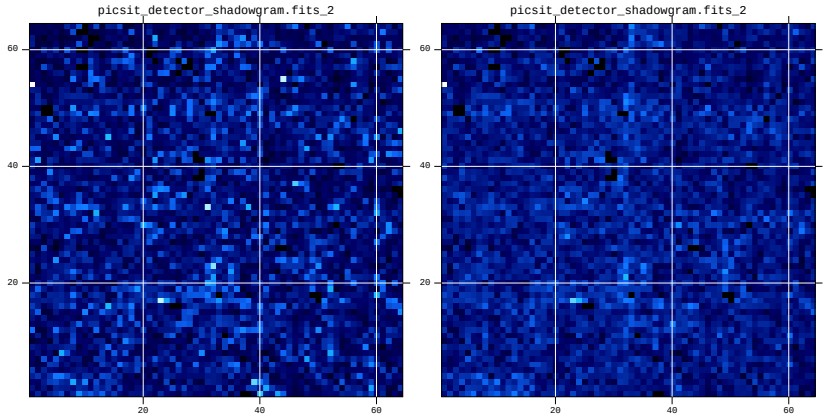

Figure 3: Effect of cosmic–rays induced events and/or noisy pixels on the shadowgrams (photon–by–photon mode). (*left*) Normal shadowgram; (*right*) Cleaned shadowgram. After the cleaning, the bright pixels disappeared. The only bright pixel remained at the top left of the cleaned shadowgram is a well–known pixel that often is hot. Data from revolution 14, energy band $170 - 250$ keV.

possible to develop an algorithm to delete from the photon list those events that can be identified as fake. After having isolated some of these "tracks", the photon list displayed series of photons "packed" in a very short time scale hitting a single pixel. Such "packets" are shown in Fig. 2, where fake events are emphasized in blue.

By removing these "packets" it is possible to obtain a cleaned shadowgram (Fig. 3), but – obviously – this is possible only when PICsIT is set to operate in photon–by–photon mode. Since the available telemetry is not sufficient for this type of mode, PICsIT works almost always in standard mode (i.e. with events integrated onboard in histograms). In this mode, there is no possibility to act on the single photon and, therefore, it is possible only to operate the *a posteriori* correction described above.

4 The sky image reconstruction

Here are shown some performances of the PICsIT ISSW. Details on the techniques of the deconvolution are available in Goldwurm et al. (2003).

4.1 Sky coordinates reconstruction

The sensitivity of PICsIT does not allow to see sources during a typical exposure of one ScW (2 ks), but there are sometimes Scw with duration of 5 ks. In this case, there is the possibility to detect the Crab at level of $SNR = 3 - 4\sigma$. During the observations of calibration performed in February 2003, the Crab was pointed during the revolutions 39, 43, 44, and 45 (staring and dithering hexagonal and 5×5). The coordinates of the Crab detected at $SNR > 3\sigma$ are reported in the Fig. 4. All the positions are within an error of $\pm 5'$ from the catalog position.

4.2 Image analysis

For the analysis with the Crab were selected the data from the revolution 39, Crab on axis, staring. The observation was about 102 ks long, but by using only the complete histograms, the effective exposure

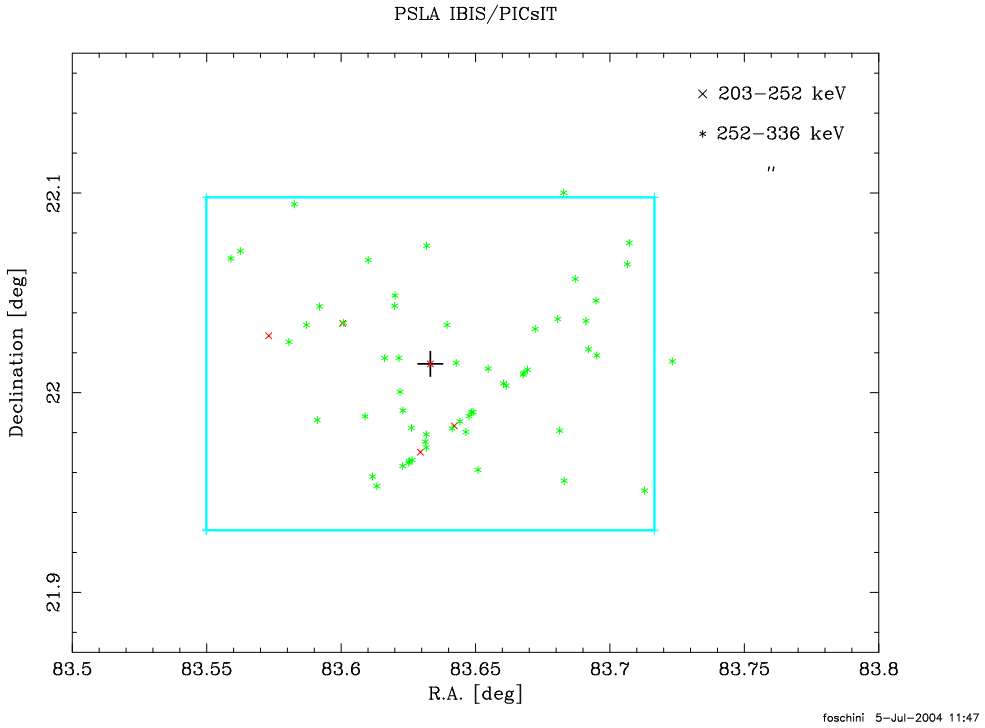

Figure 4: Sky coordinate reconstruction of the Crab position obtained with the ScW detections with $SNR > 3\sigma$ (Exposure 5 ks) in the energy band $252 - 329$ keV (*) and $203 - 252$ keV ($\times$). The catalog position of the Crab is shown at the centre of the figure and indicated with +. The surrounding square represents the pixel of PICsIT with $10'$ size.

Table 2: PICsIT observations of the Crab during Rev. 39 (staring, on axis, 77 ks) with OSA3 and OSA4. The test with OSA4 has been performed in two ways: by integrating the shadowgrams before the deconvolution with `sumhist` (I) and by deconvolving the shadowgrams every Scw and then summing them later with `ip_skymosaic` (II). Being the deconvolution a linear operation, the results should be equal, as it is (at least within the first decimal digit). Please note that OSA3 had slightly different energy bands, but the effect on the SNR and count rate is negligible. The changes shown are due to the improved background subtraction and the revision of the pipeline.

	OSA3		OSA4 I		OSA4 II	
Energy Band (keV)	Rate (c/s)	SNR (σ)	Rate (c/s)	SNR (σ)	Rate (c/s)	SNR (σ)
$203 - 252$	2.5	7.4	3.0	23.9	3.0	23.9
$252 - 336$	2.2	11.0	2.5	23.6	2.5	23.6
$336 - 448$	1.3	7.1	1.2	13.7	1.2	13.7
$448 - 672$	0.7	4.4	0.7	7.6	0.7	7.6
$672 - 1036$	–	–	0.3	4.2	0.3	4.2

reduced to 77 ks. The results are shown in the Table 2. The count rates reported here could also be considered as reference count rate for flux calibration purposes.

The best performances of PICsIT are obtained in the energy band $252 - 336$ keV, that is less affected by the cosmic–rays induced events and is in a range sufficiently low to detect enough photons. In the Fig. 5 are shown the significance maps of the observation at $252 - 336$ keV, the best detection, together with the radial profile as obtained in the OSA3 and OSA4, respectively.

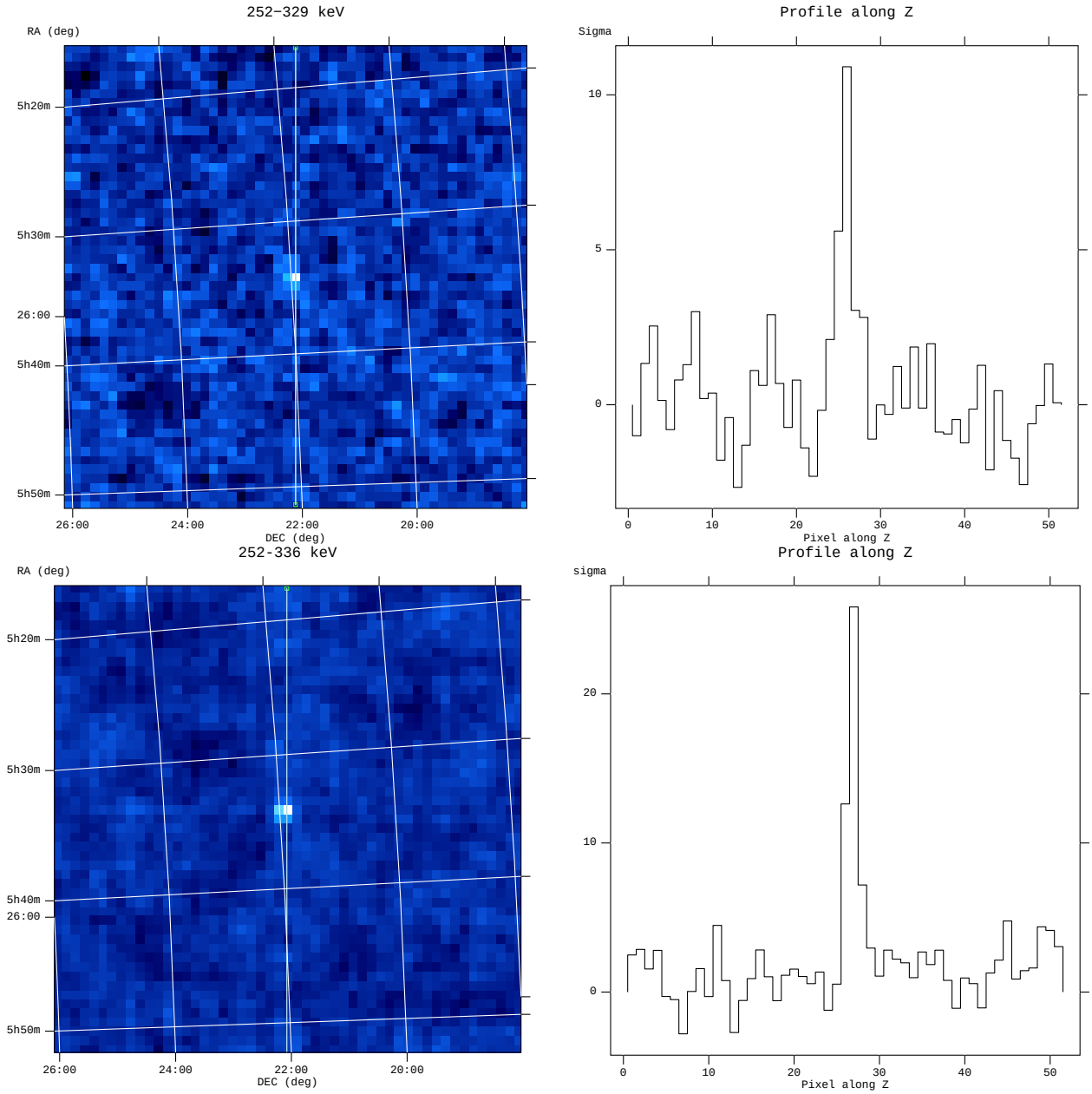

Figure 5: (*top*) Crab observation during the rev 39 (staring, on axis, 77 ks). Significance map and profile in the energy band $252 - 329$ keV. (*bottom*) The same as above, but with OSA4.

The greatest differences in the count rates and significance (for observations in staring, dithering, off axis) occur just the band $203 - 252$ keV, where we expect that the impact of cosmic–ray induced events is still high and the *a posteriori* correction – the only available since PICsIT is operated in histogram mode – may not be too much accurate (see Sect. 3.2).

It is worth mentioning that during the observations of the calibration sources some tests of the photon-by-photon mode have been set up and performed, with special telemetry allocation to PICsIT (e.g. revolutions 39 and 40). However, despite this configuration, the limited telemetry budget resulted in a loss of about 80% of the pointing time. From an observation 100 ks long at the beginning of the revolution 40, the effective exposure is only 23 ks. An inspection of the GTI table and of the lightcurve revealed that the missing time was due to telemetry gaps.

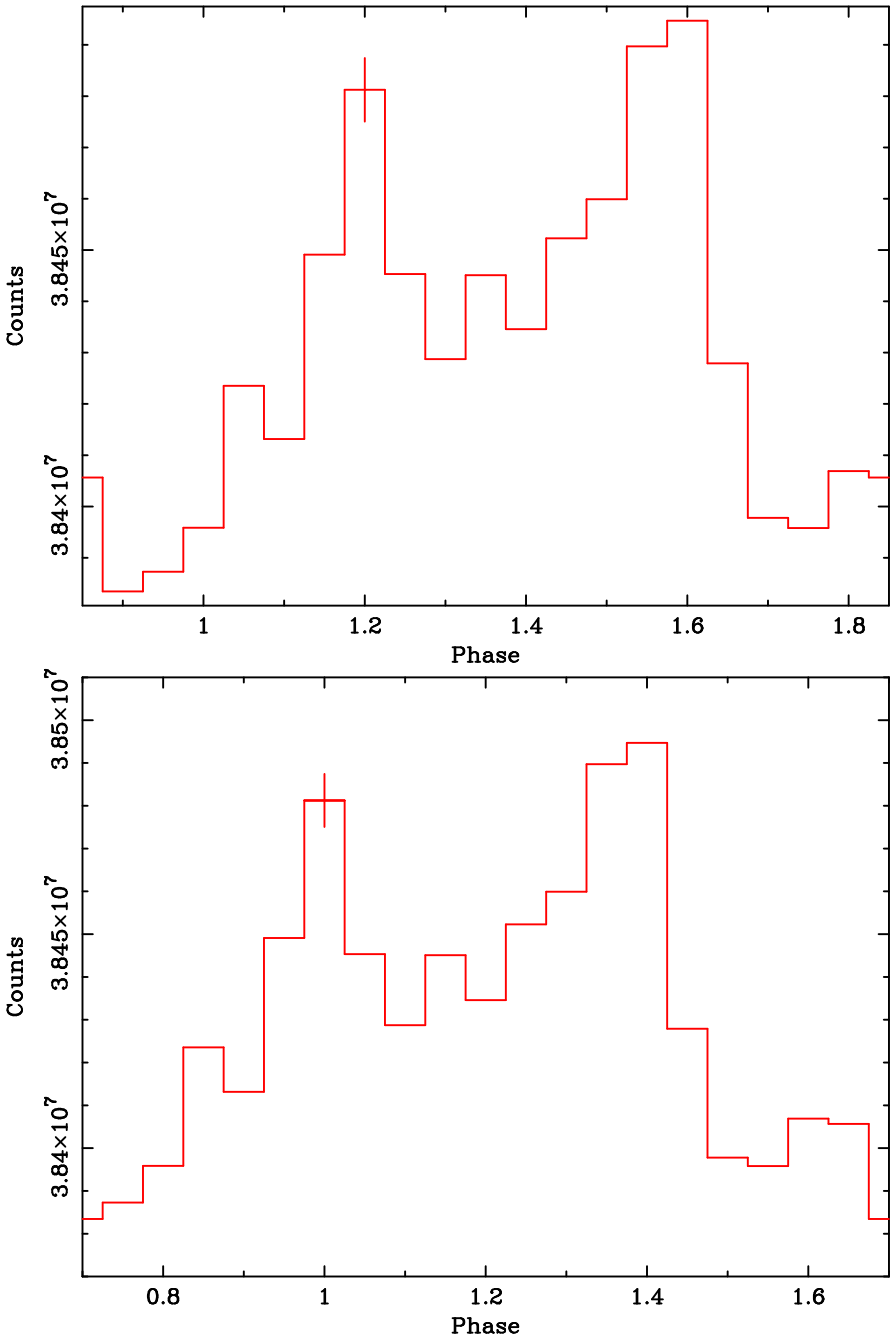

Figure 6: (*top*) Crab observation during the rev $40 - 41$ (spectral timing, 1 ms time resolution). Uncorrected folded lightcurve in the energy band $260 - 364$ keV. (*bottom*) The same as above, but corrected manually for the residual shift in phase of 0.2. Courtesy T. Mineo.

5 Timing

In February 2003, during the observation of the Crab, IBIS/PICsIT was set up to test the timing performances in the different modes of operation, i.e. photon–by–photon and spectral timing. For the moment, in the OSA, it is available the possibility to build the lightcurve for the whole detector with the spectral timing data. Therefore, we report here some tests on this part of the software, performed with the help of T. Mineo (IASF–CNR, Sezione di Palermo).

The data analysed are from the revolutions 40 and 41, with PICsIT set up in spectral timing with 1 ms time resolution and 4 energy bands ($156-208$, $208-260$, $260-364$, $364-676$ keV). The total exposure was 310 ks.

The data in output from the pipeline were corrected for barycenter with `barycent` tool of OSA. The folded lightcurve shows a shift in the phase of 0.2 (6 ms) (Fig. 6, *top*). This, for the moment, should be corrected manually (Fig. 6, *bottom*).

6 Known problems in OSA for PICsIT

Presently, these were the problem known in the OSA4 for PICsIT:

1. There is no spectral extraction yet. No RMF/ARF available. Work in progress.
2. There are some problems with `ip_skymosaic` if there are empty Scw in the observation group or Scw with only multiple events. For the moments, it is suggested to remove these scw and re-run the executable.
3. The lightcurve in spectral timing mode presents a shift of 6 ms.

Note: More informations on the in–flight performances of IBIS/PICsIT are available in the paper by Di Cocco et al. (2003). See also Malaguti et al. (2003b) for an analysis of the GRB021125. It is in preparation a report on the status of the PICsIT instrument (Di Cocco et al.).

7 References

- Calabretta M.R., Greisen E.W., 2002, A&A 395, 1077
- Courvoisier T.J.-L., Beckmann V., Bourban G., et a., 2003, A&A 411, L343
- Di Cocco G., Caroli E., Celesti E., et al., 2003, A&A 411, L189
- Ebisawa K., Bourban G., Bodaghee A., et al., 2003, A&A 411, L59
- Ferguson C., Barlow E.J., Bird A.J., et al., 2003, A&A 411, L19
- Goldwurm A., Goldoni P., Gros A., et al., 2001, In: "Exploring the gamma–ray universe. Proceedings of the Fourth INTEGRAL Workshop", 4-8 September 2000, Alicante, Spain. Editor: B. Battrick, Scientific editors: A. Gimenez, V. Reglero, and C. Winkler. ESA SP–459, p. 497.
- Goldwurm A., David P., Foschini L., et al., 2003, A&A 411, L223
- Malaguti G., Bazzano A., Bird A.J., et al., 2003a, A&A 411, L173
- Malaguti G., Bazzano A., Beckmann V., et al., 2003b, A&A 411, L307
- Natalucci L., Bird A.J., Bazzano A., et al., 2003, A&A 411, L209
- Segreto A., Labanti C., Bazzano A., et al., 2003, A&A 411, L215